Sum-over-States Calculation of the Specific Rotations of Some Substituted Oxiranes, Chloropropionitrile, Ethane, and Norbornenone

Kenneth B. Wiberg,*,† Yi-gui Wang,† Shaun M. Wilson,† Patrick H. Vaccaro,*,† and James R. Cheeseman‡

Department of Chemistry, Yale University, New Haven, Connecticut 06520-8197, and Gaussian, Inc., 340 Quinnipiac Street, Wallingford, Connecticut 06492

Received: August 25, 2006; In Final Form: October 19, 2006

A sum-over-states approach has been applied to the calculation of the specific rotations of several substituted oxiranes, 2-chloropropionitrile, and 30°-rotated ethane. In each case, the first few excited states proved to have only a relatively small effect on the calculated specific rotation. It was necessary to use a very large number of excited states in order to achieve convergence with the results of the more direct linear response method. However, the latter does not give information on which excited states are important in determining the specific rotation. Norbornenone is unique in that its greatly enhanced specific rotation as compared to norbornanone is associated with the low-energy n−π* transition. The C═C bond orbitals interact with the C═O in the LUMO, and a density difference plot for going from the ground state to the first excited state clearly shows the perturbation of the C═C.

1. Introduction

We have studied the specific rotations of a number of chiral compounds both in the gas phase and in solution[1−5] and have compared these data with the results of theoretical calculations of the specific rotations. The agreement between experiments and theory continues to improve as more advanced theoretical methods become available.[6] However, these calculations generally use the linear response method and, unfortunately, do not provide information on the contribution from different excited states to the observed rotation. It is also possible to calculate the specific rotation using a sum-over-states approach,[7] and we have now applied this method to several compounds of interest to us. It should be noted that although this method is more time-consuming than linear response,[8] it also supplies more information.

The optical activity of a chiral molecule can be described in terms of the frequency dependent electric dipole−magnetic dipole polarizability β:[9]

$$\beta = \frac{2}{3\hbar}\sum_{b\neq a}^{\infty}\frac{R_{ba}}{{\upsilon_{ba}}^2 - \upsilon^2}$$

where υ_{ba} is the rest frequency for the electronic transition, υ is the excitation frequency, and $R_{ba} = \mathrm{Im}\{\langle a|\mu^{\mathrm{E1}}|b\rangle\cdot\langle b|\mu^{\mathrm{M1}}|a\rangle\}$ is the transition rotatory strength, which couples the ground state $|a\rangle$ to an excited electronic state $|b\rangle$ under the simultaneous action of electric (μ^{E1}) and magnetic (μ^{M1}) dipole transitions. The summation is over an infinite number of excited electronic states and therefore can be thought of as a composite property, one that reflects the entire electronic distribution of the molecule. In chiroptical spectroscopy the rotatory strength plays the same role that the oscillator strength does in more conventional spectroscopic measurements. The specific rotation, [α], given in the conventional units of deg dm^{-1} (g/cm^3)$^{-1}$, is directly related to the rotatory strength by

$$[\alpha] = \frac{9143.028}{M}\cdot\sum_{b\neq a}^{\infty}\frac{\upsilon^2}{{\upsilon_{ba}}^2 - \upsilon^2}R_{ba}$$

where M is the molar mass in g/mol, υ_{ba} and υ are in any consistent energy units, and R_{ba} is in the cgs units of

$$(\times 10^{-40})\frac{\text{erg esu cm}}{\text{Gauss}}$$

Time dependent density functional theory (TDDFT) calculations[10] using the Gaussian[11] *ab initio* package provide the necessary information (R_{ba} and υ_{ba}) for each excited state to allow the calculation of the specific rotation using a sum-over-states approach. Performing the calculations in this manner on a state-by-state basis has provided new insight into the role that different excited states play, and has substantiated the fact that optical activity is indeed a composite property.

Modern electronic structure methods seldom perform the explicit summation over excited states described above, but rather rely on time-dependent linear response (LR) theory to efficiently evaluate the frequency-dependent E1−M1 polarizability tensor, $G'_{\alpha\beta}(\omega)$:[12]

$$G'_{\alpha\beta}(\omega) = \mathrm{Im}[\langle\langle\hat{\mu}_{\alpha}^{\mathrm{E1}};\hat{\mu}_{\beta}^{\mathrm{M1}}\rangle\rangle_{\omega}]$$

which provides the requisite information for ORD calculations. The general strategy is based upon economical parametrization of the electronic wavefunction, with the first-order perturbative response to external electric and magnetic fields usually being obtained through relatively straightforward solution of a coupled linear equation system.[13]

2. Substituted Oxiranes (X = F, Cl, CN, HCC)

We have studied the specific rotations of substituted oxiranes both experimentally and computationally[5] using the linear

* Authors to whom correspondence should be addressed. E-mail: kenneth.wiberg@yale.edu (K.B.W.).
† Yale University.
‡ Gaussian, Inc.

10.1021/jp0655221 CCC: $33.50
Published on Web 12/21/2006

TABLE 1: Specific Rotations of 2-Substituted Oxiranes at 589 nm

	B3LYP		
X	aug-cc-pVDZ	aug-cc-pVTZ	obs
(*S*)-F	4.6	13.3	
(*S*)-Cl	−96.2	−87.1	
(*R*)-CN	92.3	95.7	101 ± 5
(*R*)-HCC	142.4	136.6	

response formalism[6,12] with the data being summarized in Table 1. There is agreement between the specific rotations calculated at the B3LYP/aug-cc-pVDZ and aug-cc-pVTZ levels. These compounds have not previously been reported in chiral form, but we have recently been able to prepare a chiral sample of 2-cyanooxirane,[5] and its specific rotation (neat liquid) is given in Table 1. It is in agreement with the calculated value. Attempts at preparing the other substituted oxiranes are continuing.

The difference between chlorine and the other substituents is interesting. We have examined the effect of the substituents on a series of 4, 5, and 6 membered cyclic oxides, and in each case, chlorine leads to an unusual effect when it is in an anomeric position with respect to the oxygens.[5] These results will be reported in detail at a later time.

TDDFT calculations were carried out at the B3LYP/aug-cc-pVDZ level for each of the four substituted oxiranes of Table 1, and the sum-over-states results for the first 120 states are shown in Figure 1. The horizontal lines give the results of a linear response calculation using the same theoretical level. It can be seen that the calculated specific rotation changes markedly over this range of excited states, undergoing several alterations in the sign of the computed specific rotation. It is important to note the irregular effect of the first few excited states. Clearly, convergence is not achieved using the first 120 excited states.

We have extended these calculations to over 1000 states. As shown in Figure 2, after about 600 states the values settle down and finally converge to the corresponding linear response results, given by the horizontal lines.

For the sum-over-states method, either velocity-gauge or length-gauge representations may be used. In the limit of the complete basis set, the calculated value of the rotatory strength is the same for both gauge representations. As shown in Table 2, the two sum-over-states results are in good agreement with each other, suggesting that the aug-cc-pVDZ basis set may be close to basis set limit in these cases. With the DFT linear response method, the specific optical rotation is usually obtained

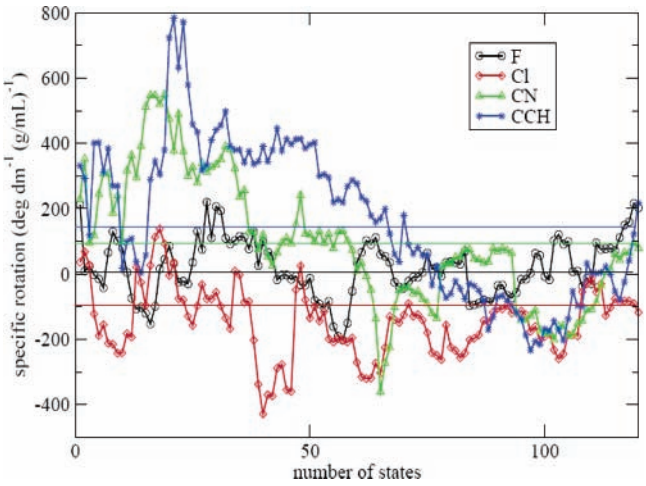

Figure 1. Results of sum-over-states calculations for oxiranes including the first 120 states. The horizontal lines give the linear response values.

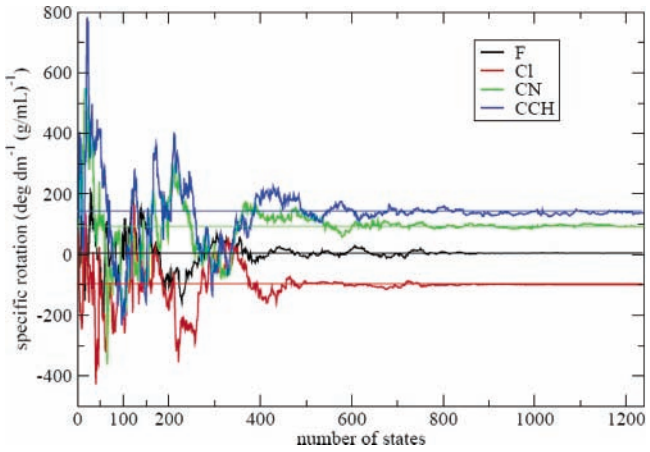

Figure 2. Extension of sum-over-states method for oxiranes to 1240 excited states.

using gauge-including atomic orbitals (GIAOs) to ensure origin independence. We have also obtained them using standard atomic orbitals for comparison. With the latest development version of Gaussian, the linear response specific rotation may also be calculated through the use of the origin-independent velocity gauge.

It can be seen that the specific rotations from the sum-over-states method using length or velocity gauge converge to those from the TDDFT method using the same gauge expressions (length or velocity). With the exception of 2-chlorooxirane, the specific rotations derived from the first excited state are much larger in magnitude than the molecular specific rotations, but the signs of the contribution from the first excited states are the same as those of the molecular specific rotations.

These results cause one to ask how many excited states are required in order to have a converged sum-over-states result? For fluorooxirane with the aug-cc-pVDZ basis set (Table 3), there are 119 basis functions, from which 119 MOs are constructed (16 occupied MOs and 103 virtual MOs). The first four MOs are from core orbitals (1s for F, O, and 2 × C) that have energies lower than −10.0 au. The energy difference between the lowest valence MO (the 5th MO) and the LUMO (the 17th MO) is about 33.4 eV, which roughly corresponds to the energy of the 480th excited state. When more than 480 excited states are included, the sum-over-states results start to converge. It is interesting that the first excited state to involve the 5th MO is the 465th excited state.

In order to see if the same effect would be found using a smaller basis set, a series of STO-3G calculations were performed (Figure S1, Table S1, and Table S2 in the Supporting Information). The energy difference between the lowest valence MO (5th MO, LVMO) and LUMO (17th MO) is near 36.6 eV, which corresponds to the energy of the 74th excited state. Although the calculated optical rotations with STO-3G basis sets are quite different than those with aug-cc-pVDZ basis sets, and the exact number of excited states is also different, the convergence condition is similar. That is, it is necessary to consider all the valence electrons in order to have converged sum-over-states results.

3. (*S*)-(−)-2-Chloropropionitrile

We have previously prepared (*S*)-(−)-2-chloropropionitrile (**1**) and have measured its chiroptical properties.[3] Calculations of the specific rotation using the linear response method and B3LYP/aug-cc-pVDZ gave values that were too large by a factor of about 2. However, the inclusion of electric field dependent

TABLE 2: The Calculated $[\alpha]_D$ for Oxiranes (X = F, Cl, CN, HCC) at the B3LYP/aug-cc-pVDZ Level

	LR-B3LYP			SOS		OR from the first ES	
X	veloc[a]	GIAO	length[a]	veloc[a]	length[a]	veloc[a]	length[a]
(*S*)-F	5.6	4.6	2.6	5.6	2.7	213.0	219.5
(*S*)-Cl	−98.0	−96.2	−96.4	−99.1	−96.9	36.3	41.2
(*R*)-CN	94.8	92.3	93.9	93.7	93.0	228.9	230.8
(*R*)-HCC	137.6	142.4	135.9	137.5	135.2	331.6	332.0

[a] GIAOs are not used in these calculations, and the velocity gauge should be gauge independent.

TABLE 3: MO Information for Oxiranes (X = F, Cl, CN, HCC) at the B3LYP/aug-cc-pVDZ Level

X	occupied	virtual	LVMO[a]	LUMO[a]	ΔE (eV)[b]	related state[c]	lowest state[d]
F	16	103	−1.23479	−0.00838	33.4	480	465
Cl	20	103	−1.12415	−0.01147	30.3	515	489
CN	18	124	−1.12862	−0.02725	30.0	615	583
HCC	18	133	−1.09736	−0.00972	29.6	695	662

[a] Energies given in hartrees. [b] The energy difference between the lowest valence MO and the LUMO. [c] Index of the excited state corresponding to the |LVMO − LUMO| gap. [d] The lowest valence MO is first involved in this excited state.

(efd) functions, which are known to markedly improve calculated polarizabilities,[14] gave specific rotations in good agreement with the experimental values.

Kowalczyk, Abrams, and Crawford (KAC)[15] have studied **1** using coupled cluster methods and found good agreement with our gas phase experimental values. They also examined the use of DFT with quite large basis sets, and found the calculated specific rotations continue to be larger than the experimental values. They concluded that the error for the DFT method is due to both underestimation of the lowest excitation energies and overestimation of the corresponding rotational strengths. They also calculated rotational strengths for the six lowest-lying excited states and found differences in both magnitude and sign, which would by themselves lead to the wrong sign for the specific rotation. In addition, they carried out a limited sum-over-states study using B3LYP/aug-cc-pVDZ (100 states) and found the result to be far from the linear response method.

Based on these findings, 2-chloropropionitrile appeared to be a good case for an extended sum-over-states study. It would be desirable to do so making use of CCSD, but unfortunately this is quite impractical at the present time. Therefore, we have made use of TDDFT calculations with B3LYP/aug-cc-pVDZ. Figure 3 gives the SOS results using the first 120 excited states. In agreement with the KAC study, the first excited state gives a positive rotation and the second gives a considerably larger negative rotation. However, the calculated rotation fluctuates wildly as the number of excited states is increased and convergence is not achieved by including just 120 excited states.

When all of the valence electrons are included (over 500 states, Figure 4), the fluctuations in the computed specific rotation become much smaller, but this property does not really converge until over 1500 states are included. Again, the SOS results converge to the linear response values (both velocity and length gauge) for all the wavelengths listed in Table 4. The SOS results from the velocity gauge are somewhat different than those from the length gauge. This might indicate that aug-cc-pVDZ has not reached the basis set limit for 2-chloropropionitrile. The specific rotations calculated with the smaller STO-3G basis set are close to those previously reported using aug-cc-pVDZ (Table S3 in the Supporting Information), and are not far from the experimental results. This finding is probably fortuitous. The SOS results using the STO-3G basis set are shown in Figure S2 in the Supporting Information.

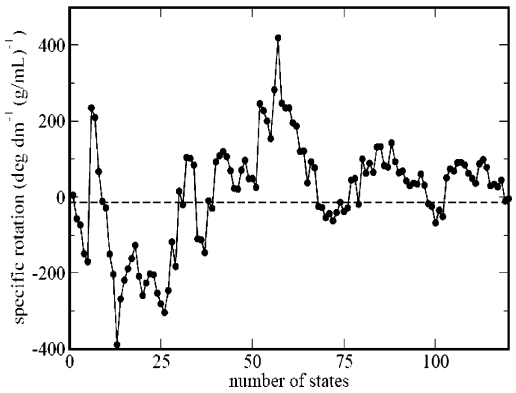

Figure 3. The SOS results for 2-chloropropionitrile with 120 states.

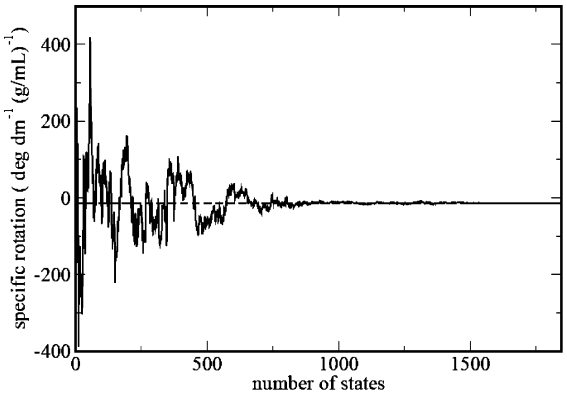

Figure 4. Extension of SOS results for 2-chloropropionitrile to over 1500 states.

It has been suggested that the frequent overestimation of optical rotation by DFT methods may come from the underestimation of the excitation energies, which is evident from the energy denominator in the equations for β and [α]. Polavarapu[16] has suggested that the TDDFT excitation energies should be increased in estimating the specific rotation. For 2-chloropropionitrile, an artificial shift of excitation energies to higher energy for every excited state by 0.6 eV as suggested by the results of KAC gives SOS values that are in better agreement with the gas phase experimental measurements (Table 4).

4. 30°-Rotated Ethane

In a study of the specific rotation of ethane with an H−C−C−H torsional angle of 30° (i.e., halfway between the staggered and eclipsed conformations), a value of $[\alpha]_D = -486$ was calculated using B3LYP/6-311++G** whereas a value of $[\alpha]_D = +41$ was calculated using B3LYP/aug-cc-pVDZ.[4] These two basis sets are of similar size and usually give comparable calculated specific rotations for most molecules.[12] The remarkable difference was traced to the inclusion of diffuse *p* functions at hydrogens in aug-cc-pVDZ whereas 6-311++G** includes only diffuse *s* functions. The addition of diffuse *p* functions to the hydrogens of the latter resulted in a calculated specific rotation that agreed with the aug-cc-pVDZ value.

The difference between the two basis sets when applied to ethane was examined using density difference plots.[4] The aug-cc-pVDZ basis led to very diffuse helical features in these plots that are probably responsible for the specific rotation. This is possible only with diffuse *p* functions on the hydrogens that have directional characteristics. It may be noted that much larger

TABLE 4: Comparison of DFT Linear Response (LR) Results with Sum-over-States Results for 2-Chloropropionitrile at the B3LYP/aug-cc-pVDZ Level (1848 States)

	LR			SOS[b]		EE + 0.6 eV[c]		expt	
nm	veloc[a]	GIAO	length[a]	veloc	length	veloc	length	gas	liquid
633	−12.1	−12.2	−11.1	−12.2	−11.3	−9.1	−8.4	−6.8±2.3	
589	−14.3	−14.5	−13.2	−14.5	−13.4	−10.8	−10.0	−8.3[d]	−14.5
436	−31.4	−31.6	−29.1	−31.8	−29.5	−23.0	−21.3	−19.8[d]	−30.9
355	−59.3	−59.1	−55.2	−59.9	−55.8	−41.8	−38.8	−37.9 ± 2.9	

[a] DFT LR results using standard atomic orbitals. [b] SOS results using TDDFT. [c] SOS results shifting the calculated transition energies (EE) by 0.6 eV. The computed vertical EEs for the first five excited states are 6.26, 6.38, 6.88, 7.29, and 7.35 eV, corresponding to absorption wavelengths of 198.0, 194.3, 180.3, 170.1, and 168.6 nm. [d] Values interpolated from 355 nm and 633 nm measurements.

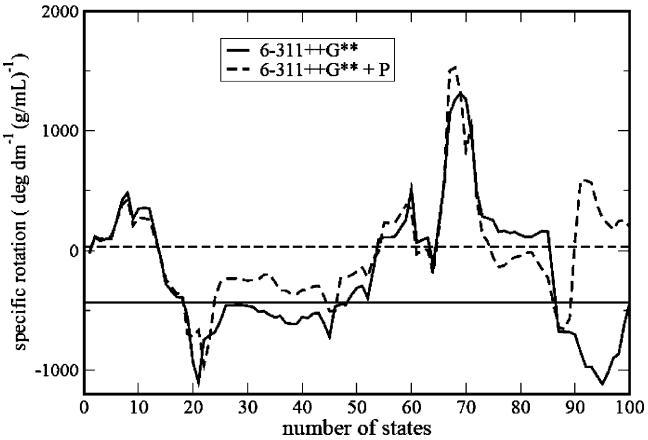

Figure 5. SOS results for 30°-rotated ethane for the first 100 excited states with B3LYP and different basis sets. Horizontal lines depict the computed linear response values for each basis set, showing the anomalous behavior found in the case of 6-311++G**.

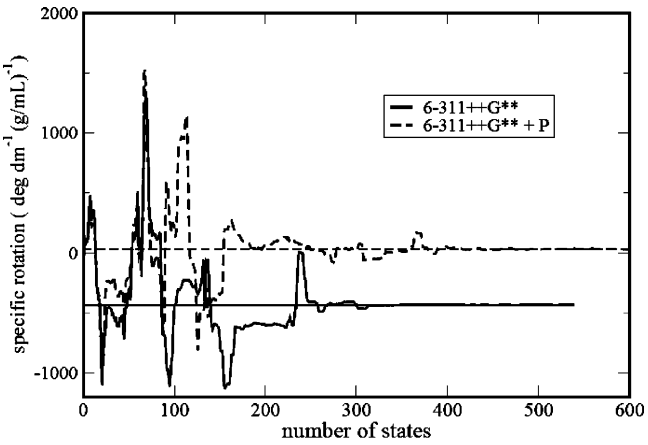

Figure 6. Extension of the SOS analysis for 30°-rotated ethane to over 500 excited states.

basis sets were examined, and the results in all cases were in good agreement with the aug-cc-pVDZ basis set.

Ethane is a small molecule, so the SOS method can use large basis sets to study many possible excited states. Figure 5 only shows the SOS results obtained for the first 100 excited states with two different basis sets. The SOS calculations appear to follow similar patterns at first, and then the 6-311++G** results diverge from those obtained with other basis sets. Two obvious departure regions are between 90−100 and 155−160 electronic states (Figures 5 and 6), in which MOs 5 and 6 and MOs 8 and 9 are the major contributors. When the plots are extended to over 500 excited states, the SOS results converge to the corresponding linear response values for all four basis sets (Figure 6 and Table 5).

The MO properties provided in Table 6 again demonstrate that it is necessary to include all valence electrons in order to have converged SOS results. The relationship between basis functions and excited states is evident here. The four types of basis sets have increasing number of basis functions (N), from which the same number of molecular orbitals (N) is constructed. Among these N molecular orbitals, the first 9 MOs are occupied and all the others are virtual ($N - 9$). Two core MOs are not involved in the excited states, so the maximum number of single-electron excited states is $(9 - 2) \times (N - 9)$.

TABLE 5: The Calculated $[\alpha]_D$ with Two Different Approaches for 30°-Rotated Ethane

	LR-B3LYP			SOS (converged)	
basis set	veloc[a]	GIAO	length[a]	veloc[a]	length[a]
6-311++G**	−657.7	−486.4	−431.7	−659.1	−432.6
6-311++G** + P[b]	12.7	41.3	32.4	12.9	32.4
aug-cc-pVDZ	19.2	41.2	31.6	19.4	31.7
aug-cc-pVTZ	51.6	53.2	52.7	51.9	52.8

[a] GIAOs were not used in these calculations. [b] 6-311++G** basis set + diffuse H p-functions from aug-cc-pVDZ (exponent 0.14).

Since the diffuse polarization functions on H have dramatic effect on optical effects, the 6-311++G** and 6-311++G** + P basis sets were examined in some detail. The converged SOS optical rotation for each occupied MO is given in Table 7. These results were obtained using the frozen window option in Gaussian that allows the calculation to use all of the excited states originating from one given occupied orbital. The sum of 1−9 is somewhat different than the linear response values (at the end of the table) because the linear combination of occupied orbitals is not included in this approach. When the molecular orbitals are studied in groups, the agreement with linear response results becomes better (such as in groups like 1−2, 3, 4, 5−9). The P functions on H produce remarkable changes for MOs 5 and 6 and MOs 8 and 9 (Table 7), and MOs 5 and 6 contribute with opposite signs than MOs 8 and 9. The final sign is determined by MOs 8 and 9. For two basis sets, the clear diverging region is from the 38th excited state to about the 52nd excited state, in which the greatest changes occur at the 39th and the 40th excited states for both pairs of MOs (Figure 7). In Table 7, the 5,6; 8,9; and 5−9 entries include these groups of occupied MOs in the frozen window. With the 6-311++G** basis set, the electronic transitions for MOs 5 and 6 are magnetically forbidden, while those for MOs 8 and 9 are electronically forbidden. This can be judged from the magnitudes of the electronic transition dipole and magnetic transition dipole (Table 8), and the inclusion of diffuse P function removes these restrictions, resulting in significant increase of rotatory strength R for these excited states. The sign of the sum of R is in agreement with those from MOs 8 and 9. A similar conclusion holds for excited states 41, 42, and 44, while the changes in magnitude of two dipoles are most likely responsible for the difference for excited states 48−52. The properties for excited states 41−52 can be found in the Supporting Information (Table S6).

TABLE 6: The MO Information for 30°-Rotated Ethane

basis sets (bf)	occ	virt	LVMO[a]	LUMO	ΔE (eV)[b]	state[c]	related[d]	no.[e]
6-311++G**(86)	9	77	−0.75300	−0.00572	20.3	125	116	539
6-311++G**+ P(104)	9	95	−0.75277	−0.00612	20.3	160	132	665
aug-cc-pVDZ(100)	9	91	−0.75368	−0.00716	20.3	164	138	637
aug-cc-pVTZ(230)	9	221	−0.75251	−0.00843	20.2	219	193	1547

[a] The energy of the lowest valence MO in eV. [b] The energy difference between the lowest valence MO and the LUMO. [c] The index of the first excited state corresponding to the |LVMO − LUMO| gap. [d] Index of the first excited state involving the lowest valence MO. [e] Maximum number of single electron excited states.

TABLE 7: The Converged SOS Optical Rotation for Each MO or a Group of MOs for 30°-Rotated Ethane

MO	6-311++G**	6-311++G** + P
1−2	0.0	0.0
3	−1.6	−1.0
4	11.3	12.7
5	173.3	−63.9
6	166.7	−56.7
7	57.5	40.5
8	−399.6	88.0
9	−503.4	67.7
sum (1−9)	−495.8	87.3
5,6	273.7	−140.5
8,9	−836.5	101.9
5−9	−441.0	23.4
LR total	−432.2	32.4

The sign of the rotatory strength for an individual excited state is determined by the angle between the corresponding transition electric-dipole (μ^{E1}) and magnetic-dipole (μ^{M1}) moments. This can be seen by recasting the expression for R_{ba} as

$$R_{ba} = \mathrm{Im}\{\langle a|\mu^{E1}|b\rangle\langle b|\mu^{M1}|a\rangle\} = |\mu_{ba}^{E1}||\mu_{ba}^{M1}|\cos\Theta_{ba}$$

where the second equality follows from the convention that matrix elements of the electric-dipole ($\mu_{ba}^{E1} = \langle b|\mu^{E1}|a\rangle$) and magnetic-dipole ($\mu_{ba}^{M1} = \langle b|\mu^{E1}|a\rangle$) operators are pure-real and pure-imaginary, respectively, for nondegenerate (pure-real) wavefunctions. These data are given in Table 8.

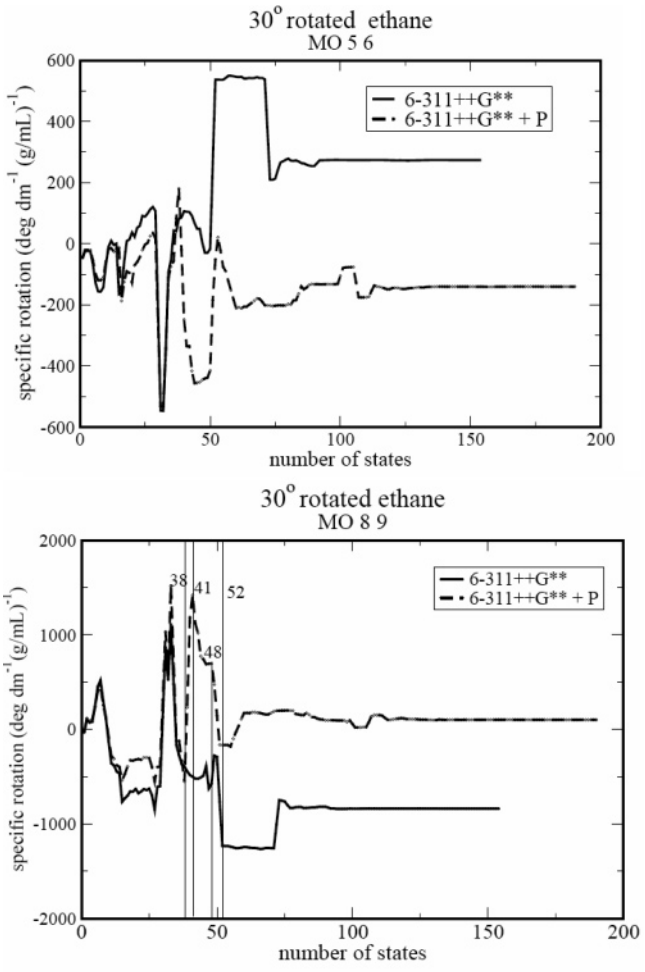

Figure 7. The SOS results for MOs 5,6 (above) and MOs 8,9 (below) in 30°-rotated ethane

TABLE 8: The Properties of Excited States 39 and 40[a]

	6-311++G**				6-311++G** + P			
	$\lvert\mu_{ba}^{E1}\rvert$	$\lvert\mu_{ba}^{M1}\rvert$	Θ_{ba}	R_{ba}	$\lvert\mu_{ba}^{E1}\rvert$	$\lvert\mu_{ba}^{M1}\rvert$	Θ_{ba}	R_{ba}
MO 5,6								
39	0.46	0.01	1.7	0.94	0.24	0.83	177.4	−47.53
40	0.45	0.05	0.2	5.36	0.26	0.90	179.9	−54.63
MO 8,9								
39	0.06	0.69	179.8	−9.94	0.77	0.77	0.2	139.05
40	0.05	0.69	170.6	−7.86	0.89	0.83	11.9	169.37

[a] Information for additional excited states may be found in the Supporting Information.

We should mention that the above analysis is a qualitative approach, and the contributions from one state can be much larger than the sum. As we can notice from Figure 7, the difference comes from a large group of states, and all of them need to be considered. Similar analyses are not possible for a group of excited states or for all the excited states at a time, because rotatory strength does not have a direction. When we compare aug-cc-pVDZ (or aug-cc-pVTZ) with 6-311++G**, the different regions are even larger though the general features are the same as those between 6-311++G** and 6-311++G** + P (Figure S4 in the Supporting Information). So we restrict our efforts to MOs 8,9 and the excited states 39, 40, 41, 42, and 44. This allows us to seek some clues from the analysis of density difference plots.

The chirality of 30°-rotated ethane comes from the orientation of the hydrogen atoms, so the correct description of them by diffuse polarization functions is crucial. The involved MOs (5,6 and 8,9) are constructed from basis functions at H, with MOs 5 and 6 have bonding character (π) while MOs 8 and 9 have antibonding (π^*) character (see Figure 8, where the colors represent the phase of the MO). The excited state characters for a few excited states in the region between 38 and 52 are given in Table S7 in the Supporting Information. For excited states 39 and 40, the mainly involved virtual orbitals are MO 29 with the 6-311++G** basis set and MO 29 and MO 30 with the 6-311++G** + P basis set (CI coefficients for involved MOs are given in Table S5 in the Supporting Information). The plots of other virtual orbitals mentioned in Table S7 can also be found in the Supporting Information. It is interesting that some MOs (MO 29 MO 33 with 6-311++G** basis sets, and MO-31-P with 6-311++G** + P basis sets) have a helical sense.

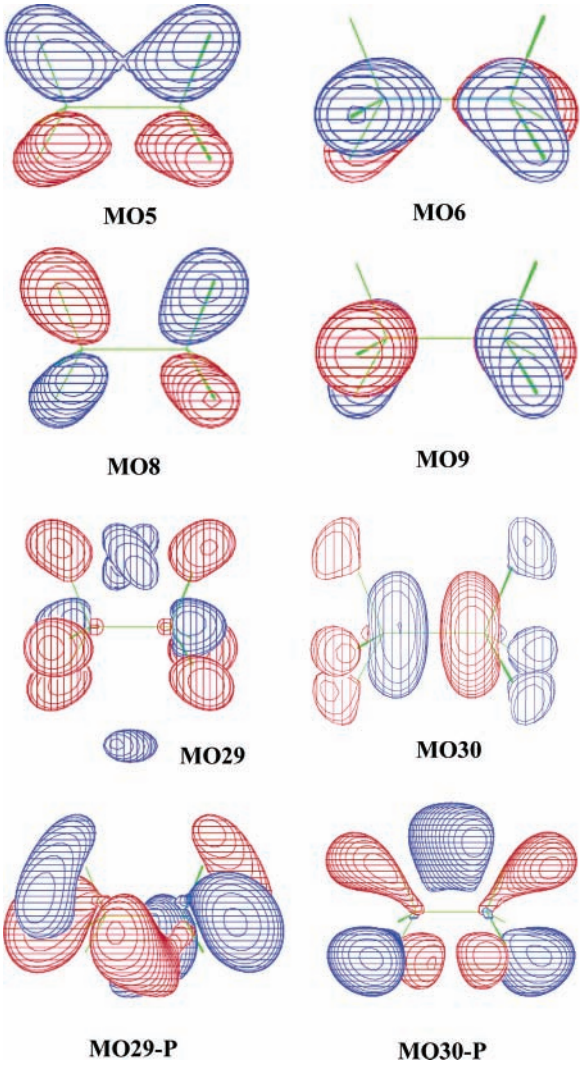

Figure 8. Plots of molecular orbitals (0.1 e/au^3 contour for occupied MOs, 0.05 e/au^3 contour for virtual MOs).

Since many virtual orbitals are involved in each excited state, it is not possible to give a very accurate conclusion only based on a few MOs or a few excited states. Thus we look at the density difference plots (shown in the Supporting Information). The helical sense can be noticed for all three basis sets in the depletion regions, and the integration values for the density difference regions are given in the Supporting Information (here blue indicates regions that have gained charge density, and red indicates regions that have been depleted). The sense of helix is the direct result of 30° rotation and *P*-functions on the hydrogen atoms.

5. (1*S*,4*S*)-Norbornenone and (1*R*,4*S*)-Norbornanone

(1*S*,4*S*)-Norbornenone (**2**) and (1*R*,4*S*)-norbornanone (**3**) differ only in that a double bond exists in the former, and this double bond is remote and perpendicular to the carbonyl group. The experimental $[\alpha]_D$ values are −1146 (in hexane)[17] and −18.19 ± 0.27 (in $HCCl_3$)[18] for (1*S*,4*S*)-norbornenone and (1*R*,4*S*)-norbornanone, respectively. A more recent report on the mirror image of **3** ((1*S*,4*R*)-norbornanone) indicates that the $[\alpha]_D^{28}$ is +29.8 (in $HCCl_3$).[19] The B3LYP/aug-cc-pVDZ values for **2** and **3** are −1221.8 and +11.3, respectively.[20] It should be noted that the specific rotation of **3** at 589 nm changes sign on going from $HCCl_3$ to isooctane (ref 17).

The effect of the first 124 states on the specific rotation are shown in Figure 9, which indicates that the first excited state

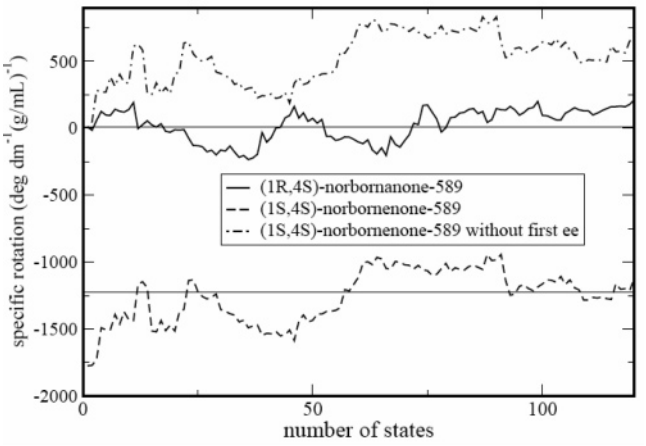

Figure 9. SOS results for (1*S*,4*S*)-norbornenone and (1*R*,4*S*)-norbornanone at B3LYP/aug-cc-pVDZ level The upper curve is for norbornenone, leaving out the contribution from the first excited state. The horizontal lines give the linear response values.

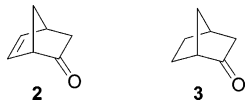

2 **3**

dominates the very large difference between these two compounds. Since the two molecules are large and the total number of excited sates for both compounds with aug-cc-pVDZ will be about 5000, we did not obtain a larger number of excited states with the aug-cc-pVDZ basis sets to get converged SOS results, but rather focused on the excited states originating from the HOMO. The SOS results are given in Figure 10. The appearance of the plots is similar to Figure 9, and it shows that the first electronic transition (mainly to the LUMO) is dominant for the total optical rotation.

The lowest excited state from the carbonyl group has n→π* character, which is magnetic-dipole allowed but nominally electric-dipole forbidden. The first excited states for the two molecules have large magnetic transition dipoles (1.15 au and 1.30 au[21] for norbornanone and norbornenone, respectively). The electronic transition dipole is small for norbornanone (0.04 au) and almost perpendicular to the magnetic dipole (the angle is 86.6°). The double bond in (1*S*,4*S*)-norbornenone increases the electronic transition dipole to 0.26 au, and in addition changes the angle to 135.0°. The double bond is involved in both the HOMO (as π) and the LUMO (as π*) of norbornenone, as shown in Figure 11, and the π→π* transition is electrically allowed. The angle between electronic transition dipole and magnetic dipole now is halfway between perpendicular and antiparallel. The first excited state is important partially because it is over 1.2 eV away from its nearest neighbor.

6. Conclusions

The computational findings presented in this paper strongly suggest that the low-lying valence and Rydberg manifolds of a chiral molecule usually are not the dominant features governing nonresonant optical activity. Instead, an unexpectedly large number of excited states are needed to converge sum-over-states calculations of specific rotation to their linear-response counterparts. This seemingly "unphysical" result can be attributed, in part, to the perturbative nature of the underlying theory,[22] with the inclusion of numerous basis functions having different spatial distributions of electron density reflecting the need to achieve requisite closure and resolution identities. Such requirements ultimately reveal inadequacies in the basis set selected

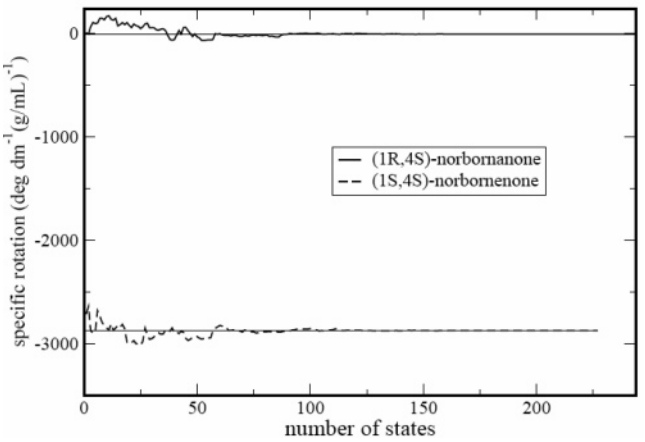

Figure 10. SOS results for the interaction of the HOMO with the exited states at the B3LYP/aug-cc-pVDZ level.

for the perturbation expansion, demonstrating the ability of canonical quantum-chemical methods to describe core-electronic features well while affording less attention to features (e.g., optical activity) that depend strongly on the "edges" of the electronic wavefunction.[23] Similar conclusions might be expected to hold for theoretical treatments of related molecular properties such as polarizability and magnetizability, which formally entail analogous sum-over-state expressions containing only electric or magnetic terms, respectively. However, the analysis of chiroptical phenomena is complicated further by the need to consider the scalar product of electric-dipole and magnetic-dipole matrix elements, each of which can possess a unique orientation in the molecular frame.

A variety of other observations support our conjecture that low-lying excited states usually are not of major importance for the quantitative evaluation of nonresonant optical activity. Evidence for this assertion can be found in Figure 12, which plots the predicted specific rotation at 589 nm ($[\alpha]_D$) for a homologous series of chiral butanes as a function of their C−C−C−C torsion angle (τ). These results follow from B3LYP/aug-cc-pVDZ optical activity calculations performed on four 2-X-butane species, where the symbol X alternately represents a fluoride (−F), chloride (−Cl), cyano (−CN), and ethynyl (−CCH) group.[2] Conformational analyses done at comparable levels of theory reveal three distinct minima on the torsional potential surface, with the *trans*-butane geometry (carbon chain in *gauche*-butane arrangement) at $\tau \approx 180°$ being straddled by two higher-energy conformers at $\tau \approx 63°$ (∼0.7 kcal/mol) and $\tau \approx 301°$ (∼0.8 kcal/mol). Despite the substantial changes in electronic characteristics imbued by the various substituents (as corroborated by recording their vacuum ultraviolet absorption spectra), the uniform pattern in Figure 12 is unmistakable, signifying a common provenance that rises above disparate details of electronic structure. Thus, it would appear that the overall "shape" of a molecule (as dominated by the *peripheral* distribution of electron density) is the key factor for determining nonresonant chiroptical properties.

While the specific rotation of a chiral molecule can be obtained through application of sum-over-state methods, convergence of the resultant quantity demands that all valence-electron excitations be considered. This typically requires a large number of excited states to be included in the perturbative expansion, thereby reinforcing the composite nature of the underlying chiroptical effects. Such behavior can be traced to the nonresonant nature of the matter-field interactions responsible for optical rotatory dispersion (ORD), with substantial detuning from resonance leading to elastic scattering processes

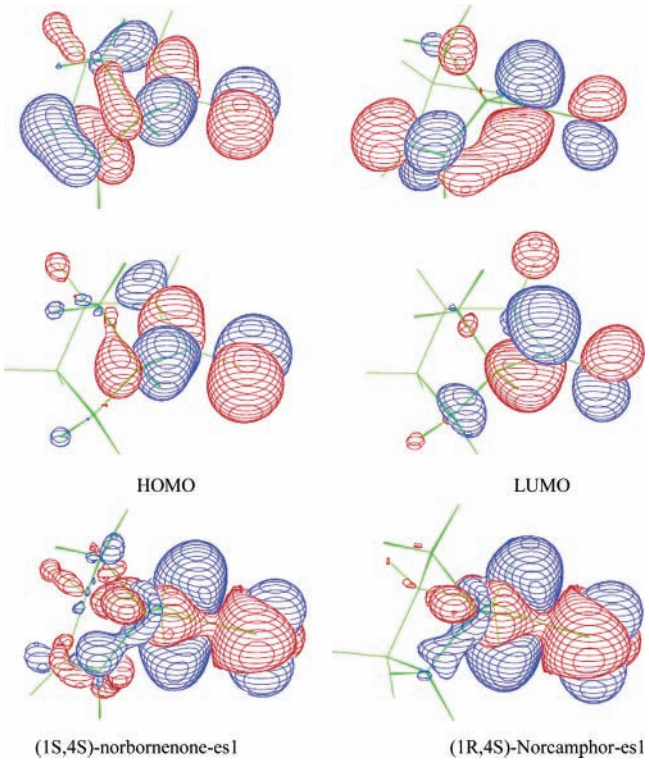

Figure 11. HOMO and LUMO (0.05 e/au^3 contour) plots (upper, norbornenone and lower, norbornanone) and density difference (0.002 e/au^3 contour) plots for going from the ground state to the first excited state.

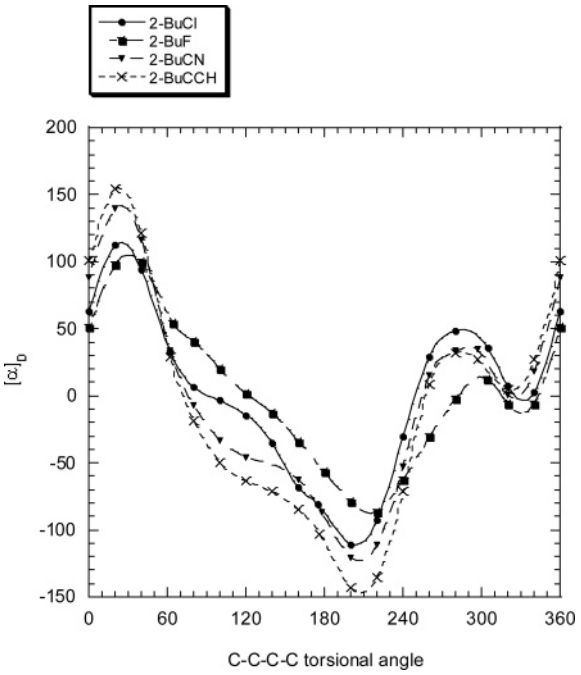

Figure 12. Calculated specific rotations for 2-substituted butane as a function of the C−C−C−C torsional angle.

that embody the dynamical response of the entire electronic distribution to oscillating electric and magnetic fields. As the incident light frequency is tuned into resonance, strong circular dichroism phenomena (whereby circular-differential absorption leads to polarization ellipticity) usually dominate over their circular birefringence counterparts (which are responsible for the polarization rotation associated with ORD). For excitations residing in the visible or ultraviolet portions of the spectrum, measurement of the resulting electronic circular dichroism

(ECD) can provide structurally localized information that reflects the proximate electronic and chemical environments for each absorbing chromophore. The properties of a single (resonant) excited state can be expected to dominate under these circumstances; however, the cooperative influence of adjacent electronic manifolds (e.g., as mediated through vibronic coupling mechanisms) often has been invoked to explain the patterns of fine structure observed in ECD spectra.[24]

Acknowledgment. This investigation was supported by grants from the National Science Foundation and the American Chemical Society Petroleum Research Fund.

Supporting Information Available: Tables of data obtained using the STO-3G basis set, and information on the properties of the excited states of 30°-rotated ethane. This material is available free of charge via the Internet at http://pubs.acs.org.

References and Notes

(1) Müller, T.; Wiberg, K. B.; Vaccaro, P. H. *J. Phys. Chem. A* **2000**, *104*, 5969. Müller, T.; Wiberg, K. B.; Vaccaro, P. H.; Cheeseman, J. R.; Frisch, M. J. *J. Opt. Soc. Am. B* **2002**, *19*, 125. Wilson, S. M.; Wiberg, K. B.; Cheeseman, J. R.; Frisch, M. J.; Vaccaro, P. H. *J. Phys. Chem. A* **2005**, *109*, 11752.

(2) Wiberg, K. B.; Wang, Y.-g.;. Vaccaro, P. H; Cheeseman, J. R.; Luderer, M. R. *J. Phys. Chem. A*, **2005**, *109*, 3405. Wiberg, K. B.; Vaccaro, P. H.; Cheeseman, J. R *J. Am. Chem. Soc*. **2003**, *125*, 1888.

(3) Wiberg, K. B.; Wang, Y.-g.; Wilson, S. M.; Vaccaro, P. H.; Cheeseman, J. R. *J. Phys. Chem. A* **2005**, *109*, 3448.

(4) Wiberg, K. B.; Wang, Y.-g.; Vaccaro, P. H.; Cheeseman, J. R.; Trucks, G.; Frisch, M. J. *J. Phys. Chem. A* **2004**, *108*, 32.

(5) Wiberg, K. B.; Wilson, S. M.; Wang, Y.-g.; Vaccaro, P. H.; Cheeseman, J. R.; Luderer, M. R. To be submitted.

(6) Crawford, T. D. *Theor. Chem. Acc.* **2006**, *115* (4), 227.

(7) A sum-over-states procedure has been applied to a number of properties such as polarizabilities, Raman optical activity, vibrational circular dichroism, and NMR spin−spin constants (Bouř, P. *Chem. Phys. Lett.* **1997**, *265*, 65; **1998**, *288*, 363. Bouř, P.; McCann, J.; Wieser, H. *J. Phys. Chem. A* **1997**, *101*, 9783. Bouř, P.; McCann, J.; Wieser, H *J. Chem. Phys.* **1998**, *108*, 8782. Bouř, P.; Buděšinsky, M. *J. Chem. Phys.* **1999**, *110*, 2836). However, in these studies the excited states were not explicitly calculated but rather were approximated using the ground state data. Qin et al. (Qin, C.-S.; Yang, G.-C.; Su, Z.-M.; Zhu, Z.-M.; Zhou, Y.-L. *Gaodeng Xuexiao Huaxue Xuebao* **2005**, *26*, 290) used a TDDFT-SOS procedure for the calculation of nonlinear optical properties of furan homologues.

(8) In the case of 2-chloropropionitrile, the sum-over-states procedure is slower than the linear response method by a factor of 3.5 (B3LYP/aug-cc-pVDZ).

(9) (a) Rosenfeld, L. *Z. Phys.* **1928**, *52*, 161. (b) Condon, E. U. *Rev. Mod. Phys.* **1937**, *9*, 432. (c) Polavarapu, P. L. *Mol. Phys.* **1997**, *91*, 551. The usual expression for β has an additional factor, c. In the SI unit sytem, c is included in the magnetic dipole transition moment.

(10) Stratmann, R. E.; Scuseria, G. E.; Frisch, M. J. *J. Chem. Phys.* **1998**, *109*, 8218 and references therein.

(11) Frisch, M. J.; Trucks, G. W.; Schlegel, H. B.; Scuseria, G. E.; Robb, M. A.; Cheeseman, J. R.; Montgomery, J. A., Jr.; Vreven, T.; Kundin, K. N.; Burant, J. C.; Millam, J. M.; Iyengar, S. S.; Tomasi, J.; Barone, V.; Mennucci, B.; Cossi, M.; Scalmani, G.; Rega, N.; Petersson, G. A.; Nakatsuji, H.; Hada, M.; Ehara, M.; Toyota, K.; Fukuda, R.; Hasegawa, J.; Ishida, M.; Nakajima, T.; Honda, Y.; Kitao, O.; Nakai, H.; Klene, M.; Li, X.; Knox, J. E.; Hratchian, H. P.; Cross, J. B.; Adamo, C.; Jaramillo, J.; Gomperts, R; Stratmann, R. E.; Yazyev, O.; Austin, A. J.; Cammi, R.; Pomelli, C.; Ochterski, J. W.; Ayala, P. Y.; Morokuma, K.; Voth, G. A.; Salvador, P.; Dannenberg, J. J.; Zakrzewski, V. G.; Dapprich, S.; Daniels, A. D.; Strain, M. C.; Farkas, O.; Malick, D. K.; Rabuck, A. D.; Raghavachari, K.; Foresman, J. B.; Ortis, J. V.; Cui, Q.; Baboul, A. G.; Clifford, S.; Cioslowski, J.; Stefanov, B. B.; Liu, G.; Liashenko, A.; Piskorz, P.; Komaromi, I.;. Martin, R. L.; Fox, D. J.; Keith, T.; Al-Laham, M. A.; Peng, C. Y.; Nanayakkara, A.; Challacombe, M.; Gill, P. M. W.; Johnson, B.; Chen, W.; Wong, M. W.; Gonzalez, C.; Pople, J. A. *Gaussian Development version E*; Gaussian, Inc.: Wallingford, CT, 2006.

(12) DFT implementation: Stephens, P. J.; Devlin, F. J.; Cheeseman, J. R.; Frisch, M. J. *J. Phys. Chem. A* **2001**, *105*, 5356.

(13) Olsen, J.; Jørgensen, P. *J. Chem. Phys.* **1985**, *82* (7), 3235−3264. Jørgensen, P.; Jensen, H. J. A.; Olsen, J. *J. Chem. Phys.* **1988**, *89* (6), 3654−3661.

(14) Darling, C. L.; Schlegel, H. B. *J. Phys. Chem.* **1994**, *98*, 5855.

(15) Kowalczyk, T. D.; Abrams, M. L.; Crawford, T. D. *J. Phys. Chem.* **2006**, *110*, 7649.

(16) Polavarapu, P. L. *J. Phys. Chem. A* **2005**, *109*, 7013.

(17) Sandman, D. J.; Mislow, K. *J. Org. Chem.* **1968**, *33*, 2924. Lightner, D. A.; Gawronski, J. K.; Bouman, T. D. *J. Am. Chem. Soc.* **1980**, *102*, 5749.

(18) McDonald, R. N.; Steppel, R. N. *J. Am. Chem. Soc.* **1970**, *92*, 5664.

(19) Kawamura, M.; Ogasawara, K. *Tetrahedron Lett.* **1995**, *36*, 3369.

(20) Values obtained in this laboratory using B3LYP/6-311++G** optimized structures. Slightly different values were reported in ref 12 and by Stephens et al. (Stephens, P. J.; McCann, D. M.; Cheeseman, J. R.; Frisch, M. J. *Chirality* **2005**, *17*, S52).

(21) It should be noted that the output of Gaussian for the electric and magnetic dipole transition moments is given in atomic units. To convert between atomic units and SI units one uses the following conversion factors: 1 atomic unit of electric dipole transition moment = 8.47835309 $\times$ 10^{-30} C m; 1 atomic unit of magnetic dipole transition moment = 1.85480190 $\times$ 10^{-23} J/T. For example, if the magnetic dipole transition moment has a value of 1.15 au and the electric dipole transition moment has a value of 0.04 au, then their values in SI units are 1.15 au $\times$ [(1.85480190 $\times$ 10^{-23})(J/T)]/(1 au) = 2.13 $\times$ 10^{-23} J/T and 0.04 au $\times$ (8.47835309 $\times$ 10^{-30} C m)/(1 au) = 3.39 $\times$ 10^{-31} C m.

(22) Baron, L. D. *Molecular Light Scattering and Optical Activity*; Cambridge Univ. Press: Cambridge, 2004. Wagnière, G. H. *Linear and Nonlinear Properties of Molecules*; VCH Publishers: New York, 1993.

(23) Dykstra, C. E.; Liu, S. Y.; Malic, D. J. *Adv. Chem. Phys.* **1989**, *75*, 37. Hudis, J. A.; Ditchfield, R. *Chem. Phys.* **1984**, *86*, 455. Sadlej, A. J. *Chem. Phys. Lett.* **1977**, *47*, 50.

(24) Nooijen, M. *Int. J. Quantum Chem.* 2006, 106, 2489. Dierksen, M.; Grimme, S. *J. Chem. Phys.* **2006**, *124*, 174301. Neugebauer, J.; Jan Baerends, E.; Nooijen, M.; Autschbach, J. *J. Chem. Phys.* **2005**, *122*, 234305. Dewey, T. G. *J. Chem. Phys.* **1985**, *83*, 486.